AD

TECHNICAL REPORT ARCCB-TR-90016

A PLANE-STRAIN ELASTIC STRESS SOLUTION FOR A MULTIORTHOTROPIC-LAYERED CYLINDER

MARK D. WITHERELL

JUNE 1990

US ARMY ARMAMENT RESEARCH,
DEVELOPMENT AND ENGINEERING CENTER
CLOSE COMBAT ARMAMENTS CENTER
BENÉT LABORATORIES
WATERVLIET, N.Y. 12189-4050

APPROVED FOR PUBLIC RELEASE; DISTRIBUTION UNLIMITED

DISCLAIMER

The findings in this report are not to be construed as an official Department of the Army position unless so designated by other authorized documents.

The use of trade name(s) and/or manufacturer(s) does not constitute an official indorsement or approval.

DESTRUCTION NOTICE

For classified documents, follow the procedures in DoD 5200.22-M, Industrial Security Manual, Section II-19 or DoD 5200.1-R, Information Security Program Regulation, Chapter IX.

For unclassified, limited documents, destroy by any method that will prevent disclosure of contents or reconstruction of the document.

For unclassified, unlimited documents, destroy when the report is no longer needed. Do not return it to the originator.

SECURITY CLASSIFICATION OF THIS PAGE (When Data Entered)

REPORT DOCUMENTATION PAGE		READ INSTRUCTIONS BEFORE COMPLETING FORM
1. REPORT NUMBER ARCCB-TR-90016	2. GOVT ACCESSION NO.	3. RECIPIENT'S CATALOG NUMBER
4. TITLE (and Subtitle) A PLANE-STRAIN ELASTIC STRESS SOLUTION FOR A MULTIORTHOTROPIC-LAYERED CYLINDER		5. TYPE OF REPORT & PERIOD COVERED Final 6. PERFORMING ORG. REPORT NUMBER
7. AUTHOR(s) Mark D. Witherell		8. CONTRACT OR GRANT NUMBER(s)
9. PERFORMING ORGANIZATION NAME AND ADDRESS U.S. Army ARDEC Benet Laboratories, SMCAR-CCB-TL Watervliet, NY 12189-4050		10. PROGRAM ELEMENT, PROJECT, TASK AREA & WORK UNIT NUMBERS AMCMS No. 6126.23.1BL0.0 PRON No. 1A72ZH3HNMSC
11. CONTROLLING OFFICE NAME AND ADDRESS U.S. Army ARDEC Close Combat Armaments Center Picatinny Arsenal, NJ 07806-5000		12. REPORT DATE June 1990 13. NUMBER OF PAGES 24
14. MONITORING AGENCY NAME & ADDRESS(if different from Controlling Office)		15. SECURITY CLASS. (of this report) UNCLASSIFIED 15a. DECLASSIFICATION/DOWNGRADING SCHEDULE

16. DISTRIBUTION STATEMENT (of this Report)

Approved for public release; distribution unlimited.

17. DISTRIBUTION STATEMENT (of the abstract entered in Block 20, if different from Report)

18. SUPPLEMENTARY NOTES

19. KEY WORDS (Continue on reverse side if necessary and identify by block number)

Stress Distribution
Orthotropic
Multilayered
Cylinder
Composite

20. ABSTRACT (Continue on reverse side if necessary and identify by block number)

In 1963 Lekhnitskii published the equations that describe the distribution of stresses in a monolayered anisotropic cylinder under the influence of various loading conditions. Recently, O'Hara simplified these equations for the case of an orthotropic cylinder and cast them into a form that is convenient to use. This report discusses the methodology of constructing the stress solution for a multiorthotropic-layered cylinder under plane-strain boundary conditions, i.e., all orthotropic layers have zero axial strain. Combined

(CONT'D ON REVERSE)

DD FORM 1 JAN 73 1473 EDITION OF 1 NOV 65 IS OBSOLETE

UNCLASSIFIED

SECURITY CLASSIFICATION OF THIS PAGE (When Data Entered)

20. ABSTRACT (CONT'D)

loadings of internal and external pressure are allowed. Solutions for a selected layup and loading conditions are compared with finite element results and show excellent agreement. In addition, a procedure to obtain the stress solution when an interference exists at the interface of two orthotropic layers is discussed.

TABLE OF CONTENTS

TABLES

LIST OF ILLUSTRATIONS

Page

NOMENCLATURE

a - inner radius of orthotropic layer

$[A]$ - the material compliance matrix

b - outer radius of orthotropic layer

C_o - ratio of inner to outer radius of orthotropic layer ($C_o = a/b$)

E_r, E_θ, E_z - engineering modulii of orthotropic layer

FZ - axial force on orthotropic layer to enforce plane-strain boundary counditions

FZP - layer axial force contribution per unit of internal pressure

FZQ - layer axial force contribution per unit of external pressure

FZT - total axial force on multiorthotropic-layered cylinder to enforce plane-strain boundary conditions

G_{ij} - material-geometry constant from hoop strain equivalence condition ($1 \leq i \leq N-1$, $1 \leq j \leq 3$)

$[J]$ - matrix of G_{ij} values correctly positioned

$[JI]$ - inverse of $[J]$

k - orthotropic material parameter

N - total number of layers in multilayered cylinder

p - internal pressure on layer

$[Q]$ - unknown external pressure vector

P_I - interference pressure

q - external pressure on layer

r - radius

$[R]$ - result vector

RAP,TAP,ZAP - magnitude of r,θ,z stresses evaluated at r=a, caused by unit internal pressure

RAQ,TAQ,ZAQ - magnitude of r,θ,z stresses evaluated at r=a, caused by unit external pressure

RBP,TBP,ZBP - magnitude of r,θ,z stresses evaluated at r=b, caused by unit internal pressure

RBQ,TBQ,ZBQ - magnitude of r,θ,z stresses evaluated at r=b, caused by unit external pressure

β_{ij} - compliance for cylindrical problem

δ - radial interference of two multilayered cylinders

δ_i - decrease in outer radius 'b' of inner cylinder per unit of external pressure (interference loading case)

δ_o - increase in inner radius 'a' of outer cylinder per unit of internal pressure (interference loading case)

δ_u - radial interference reduction per unit pressure at interface of two multiorthotropic-layered cylinders

ϵ - strain

$\nu_{r\theta}, \nu_{\theta z}, \nu_{zr}$ - Poisson's ratio of orthotropic layer (e.g., $\nu_{r\theta} = \left| \frac{\epsilon_\theta}{\epsilon_r} \right|$, r-stress producing contraction in θ-direction)

σ - stress

[ ] - matrix of values

(i) - pertaining to i^{th} orthotropic layer

Subscripts

a,b - inner and outer radial evaluation points

r,θ,z - radial, hoop, and axial directions

1,2,3 - directions for orthogonal coordinate system (for a cylindrical system 1,2,3 correspond to r,θ,z directions)

INTRODUCTION

The attractiveness of many composite materials is their high specific stiffness making them an ideal choice for lightweight applications. In order to effectively design cylinders that incorporate composites, it is important to be able to predict the stress distribution caused by various loadings applied to the cylinder. In the early 1960s, Lehknitskii (ref 1) published a generalized plane-strain stress solution for a monolayered anisotropic cylinder under combined loadings of internal pressure, external pressure, and axial force. More recently, O'Hara (ref 2) simplified these equations for the special case of an orthotropic material and cast them in a form that is convenient to use. In real applications, however, composite cylinders are often constructed by winding fibers or laying up fibers at various angles. Generally, the cylinder is constructed by building up fiber windings in positive and negative wrap angle pairs. Each of these positive and negative wrap angle pairs can be viewed as a single orthotropic layer. The whole structure can be considered a multi-orthotropic-layered cylinder. For these types of multilayered cylinders, it becomes important to be able to obtain the stress distribution so that design and analysis can be pursued. By using Lehknitskii's monolayered solution and the proper boundary conditions, the multilayered solution can be constructed. The equations presented herein are for a multiorthotropic-layered cylinder under plane-strain boundary conditions with internal pressure, external pressure, and interference loadings.

GEOMETRY

A multilayered cylinder can be viewed as an assembly of many single-layered cylinders. It is fitting, therefore, to begin with a review of the geometry of the monolayered cylinder problem.

For the monolayered case, the cylinder is assumed to be long with ends that are fixed (see Figure 1). The fixed-end condition implies zero axial strain through the radial thickness of the cylinder. The cylinder has an inner radius 'a' and an outer radius 'b'. A cylindrically orthotropic material is assumed with its principal axes coincident with the cylinder. Orthotropic material, in general, is characterized by nine independent material constants. These constants consist of three engineering modulii (E_1,E_2,E_3), three shear modulii (G_{12},G_{23},G_{31}), and three Poisson's ratios (ν_{12},ν_{23},ν_{31}). The numbers 1,2,3 indicate the principal material directions. For the above assumptions, the 1,2,3 directions correspond to the radial, hoop, and axial directions of the cylinder (r,θ,z). The cylinder can be subjected to internal pressure 'p' and external pressure 'q'. In addition, since the principal stress directions correspond to the principal geometry directions of both the cylinder and the applied loadings, shear effects are eliminated.

STRESS EQUATIONS FOR MONOLAYERED ORTHOTROPIC CYLINDER

Lekhnitskii's solution (ref 1) for a cylinder with one anisotropic layer can be simplified for the case when the material is orthotropic. This simplification was done by O'Hara (ref 2) and resulted in three stress equations that correspond to the r,θ,z directions and one equation that predicts the axial force necessary to enforce the fixed-end constraint. These equations are given below and are identical to those found in Reference 2 with one correction for a typographical error in the σ_z equation. Also, the axial force name has been changed from PP to FZ for clarity.

$$\sigma_r = \left[\frac{pC_o^{k+1} - q}{(1-C_o^{2k})}\right]\left(\frac{r}{b}\right)^{k-1} + \left[\frac{qC_o^{k-1} - p}{(1-C_o^{2k})}\right]C_o^{k+1}\left(\frac{b}{r}\right)^{k+1} \qquad (1)$$

$$\sigma_\theta = \left[\frac{pC_o^{k+1} - q}{(1-C_o^{2k})} \right] k\left(\frac{r}{b}\right)^{k-1} - \left[\frac{qC_o^{k-1} - p}{(1-C_o^{2k})} \right] kC_o^{k+1}\left(\frac{b}{r}\right)^{k+1} \tag{2}$$

$$\sigma_z = \frac{-1}{A_{33}} \left[\left[\frac{pC_o^{k+1} - q}{(1-C_o^{2k})} \right] (A_{13}+kA_{23})\left(\frac{r}{b}\right)^{k-1} + \left[\frac{qC_o^{k-1} - p}{(1-C_o^{2k})} \right] (A_{13}-kA_{23})C_o^{k+1}\left(\frac{b}{r}\right)^{k+1} \right] \tag{3}$$

$$FZ = \frac{2\pi}{A_{33}(1-C_o^{2k})} \left[b^2(q-pC_o^{k+1})(1-C_o^{k+1}) \frac{A_{13} + kA_{23}}{1 + k} \right.$$

$$\left. + a^2(qC_o^{k-1}-p)(1-C_o^{k-1}) \frac{A_{13} - kA_{23}}{1 - k} \right] \tag{4}$$

where 'r' is the radial position in the cylinder,

$$C_o = \frac{a}{b} \tag{5}$$

and the components A_{ij} are the elements of the compliance matrix as given in Hooke's Law,

$$[\epsilon] = [A]\ [\sigma] \tag{6}$$

'k' is an orthotropic material constant given by

$$k = \sqrt{\frac{\beta_{11}}{\beta_{22}}} \tag{7}$$

where, in general,

$$\beta_{ij} = A_{ij} - \frac{A_{i3}\ A_{3j}}{A_{33}} \tag{8}$$

In developing the multilayered solution, applying the correct boundary conditions at the interface of two orthotropic layers necessitates the use of stress values evaluated at the inner (r=a) and outer (r=b) surfaces of each layer. This evaluation process leads to the six stress equations given below.

Stress Equations Evaluated at Inner Radius (r=a)

$$\sigma_{r,a} = RAP \cdot p + RAQ \cdot q \tag{9}$$

$$RAP = -1 \quad , \quad RAQ = 0$$

$$\sigma_{\theta,a} = TAP \cdot p + TAQ \cdot q \tag{10}$$

$$TAP = \frac{k(1+C_o^{2k})}{(1-C_o^{2k})} \quad , \quad TAQ = \frac{-2kC_o^{k-1}}{(1-C_o^{2k})}$$

$$\sigma_{z,a} = ZAP \cdot p + ZAQ \cdot q \tag{11}$$

$$ZAP = \frac{(A_{13}-A_{23} \cdot TAP)}{A_{33}} \quad , \quad ZAQ = \frac{-A_{23} \cdot TAQ}{A_{33}}$$

Stress Equations Evaluated at Outer Radius (r=b)

$$\sigma_{r,b} = RBP \cdot p + RBQ \cdot q \tag{12}$$

$$RBP = 0 \quad , \quad RBQ = -1$$

$$\sigma_{\theta,b} = TBP \cdot p + TBQ \cdot q \tag{13}$$

$$TBP = -TAQ \cdot C_o^2 \quad , \quad TBQ = -TAP$$

$$\sigma_{z,b} = ZBP \cdot p + ZBQ \cdot q \tag{14}$$

$$ZBP = -ZAQ \cdot C_o^2 \quad , \quad ZBQ = -ZAP + \frac{2A_{13}}{A_{33}}$$

Also, the axial force equation can be rewritten in a similiar form.

$$FZ = FZP \cdot p + FZQ \cdot q \tag{15}$$

$$FZP = \frac{2\pi a^2}{A_{33}} \left[\frac{[(TAP+TAQ+1)(A_{23}-A_{13})]}{(1-k^2)} - A_{23} \right]$$

$$FZQ = -\frac{2\pi b^2}{A_{33}} \left[\frac{[(TBP+TBQ+1)(A_{23}-A_{13})]}{(1-k^2)} - A_{23} \right]$$

In each of the six stress equations above, there are two constants (e.g., TAP, TAQ) which determine the magnitude of the contribution to the given stress caused by the internal and external pressure. These constants are material- and geometry-dependent, and each has a three-letter name. The first letter corresponds to the stress direction (r,θ,z), the second letter signifies the point at which the stress has been evaluated (a,b), and the third letter corresponds to the pressure it applies (q,p). For example, TAQ is the constant for the Theta stress, evaluated at r = a (A), magnifying the external pressure q (Q).

STRESS SOLUTION FOR MULTIORTHOTROPIC-LAYERED CYLINDER

In this section the methodology of constructing the stress solution for a multilayered cylinder (see Figure 2) is discussed where each layer has material and geometry definitions identical to those discussed for the monolayered case.

The first step to construct the multilayered solution is to equate the circumferential (hoop) strain of adjacent orthotropic layers at their interface. In other words, we equate the hoop strain at r=b of the i^{th} layer with the hoop strain at r=a of the i+1 layer

$$\epsilon_{\theta,b}(i) = \epsilon_{\theta,a}(i+1) \tag{16a}$$

Recalling that $[\epsilon] = [A]\,[\sigma]$ and that 1,2,3 correspond to the r,θ,z directions

$$\epsilon_{2,b}(i) = \epsilon_{2,a}(i+1) \tag{16b}$$

or

$$A_{12}(i)\cdot\sigma_{r,b}(i) + A_{22}(i)\cdot\sigma_{\theta,b}(i) + A_{23}\cdot\sigma_{z,b}(i) =$$

$$A_{12}(i+1)\cdot\sigma_{r,a}(i+1) + A_{22}(i+1)\cdot\sigma_{\theta,a}(i+1) + A_{23}\cdot\sigma_{z,a}(i+1) \tag{17}$$

Now, substituting the expressions for stress found in Eqs. (9) through (14) we have

$$-A_{12}(i)\cdot q(i) + A_{22}(i)\cdot[TBQ(i)\cdot q(i) + TBP(i)\cdot p(i)] +$$

$$A_{23}(i)\cdot[ZBQ(i)\cdot q(i) + ZBP(i)\cdot p(i)] =$$

$$-A_{12}(i+1)\cdot p(i+1) + A_{22}(i+1)\cdot[TAQ(i+1)\cdot q(i+1) + TAP(i+1)\cdot p(i+1)] +$$

$$A_{23}(i+1)\cdot[ZAQ(i+1)\cdot q(i+1) + ZAP(i+1)\cdot p(i+1)] \tag{18}$$

Rearranging and noting from equilibrium conditions that

$$p(i) = q(i-1) \tag{19}$$

we have

$$G_{i1}\cdot q(i-1) + G_{i2}\cdot q(i) + G_{i3}\cdot q(i+1) = 0 \tag{20}$$

where

$$G_{i1} = -C_o^2(i)\cdot\beta_{22}(i)\cdot TAQ(i)$$

$$G_{i2} = -[\beta_{12}(i) - \beta_{12}(i+1) + \beta_{22}(i)\cdot TAP(i) + \beta_{22}(i+1)\cdot TAP(i+1)]$$

$$G_{i3} = -\beta_{22}(i+1)\cdot TAQ(i+1)$$

For each two-layer combination there is one equation defining the hoop strain equivalence condition. For a cylinder with 'N' orthotropic layers there are N-1 equations and N-1 unknowns. Setting up these equations in matrix form gives the following:

$$\begin{bmatrix} G_{11} & G_{12} & G_{13} & & & & & \\ & G_{21} & G_{22} & G_{23} & & & 0 & \\ & & G_{31} & G_{32} & G_{33} & & & \\ & & & - & - & - & & \\ & & & & - & - & - & \\ & & & & & \cdot & & \\ & & & & & \cdot & & \\ & & & & & \cdot & & \\ 0 & & & & & - & - & - \\ & & & & & & G_{N-1,1} & G_{N-1,2} & G_{N-1,3} \end{bmatrix} \cdot \begin{bmatrix} q(0) \\ q(1) \\ q(2) \\ \cdot \\ \cdot \\ \cdot \\ \cdot \\ \cdot \\ \cdot \\ \cdot \\ q(N) \end{bmatrix} = 0 \qquad (21)$$

Since q(0) and q(N) are simply the internal and external pressure of the overall cylinder and are known quantities, the above matrix expression reduces to

$$\begin{bmatrix} G_{12} & G_{13} & & & & & \\ G_{21} & G_{22} & G_{23} & & & 0 & \\ & G_{31} & G_{32} & G_{33} & & & \\ & & - & - & - & & \\ & & & - & - & - & \\ & & & & \cdot & & \\ & & & & \cdot & & \\ & & & & \cdot & & \\ 0 & & & & G_{N-2,1} & G_{N-2,2} & G_{N-2,3} \\ & & & & & G_{N-1,1} & G_{N-1,2} \end{bmatrix} \begin{bmatrix} q(1) \\ q(2) \\ q(3) \\ \cdot \\ \cdot \\ \cdot \\ \cdot \\ \cdot \\ \cdot \\ \cdot \\ q(N-1) \end{bmatrix} = \begin{bmatrix} -G_{11} \cdot p(1) \\ 0 \\ 0 \\ \cdot \\ \cdot \\ \cdot \\ \cdot \\ \cdot \\ \cdot \\ \cdot \\ -G_{N-1,3} \cdot q(N) \end{bmatrix} \qquad (22)$$

or

$$[J]\,[Q] = [R] \qquad (23)$$

Solving for the matrix [Q] we have

$$[Q] = [J]^{-1}\,[R] = [JI]\,[R] \qquad (24)$$

where

$$[JI] = [J]^{-1} \qquad (25)$$

Once [JI] is determined, the interface pressures can be found easily by the following equation:

For $(1 \leq i \leq N-1)$:

$$q(i) = -JI_{i,1} \cdot G_{11} \cdot p(1) - JI_{i,N-1} \cdot G_{N-1,3} \cdot q(N) \tag{26}$$

By recalling that $p(i) = q(i-1)$, we can now calculate the stress distribution in each layer by using the general stress equations (Eqs. (1) through (4)) with p(i) and q(i) as input.

In addition to finding the stress distribution in each layer, the axial force necessary to constrain each layer to zero axial strain can be calculated using Eq. (15) with p(i) and q(i) as input. By summing the axial forces on each layer, we can determine the total axial force, FZT, on the multilayered cylinder

$$FZT = \sum_{i=1}^{N} FZ(i) \tag{27}$$

MULTILAYERED SOLUTION FOR PRESS AND SHRINK FIT

For many engineering applications, it is desirable to assemble two cylinders by shrinking or press fitting one part upon the other. This process produces a pressure at the mating surface of the two vessels. The stresses resulting from this pressure on each cylinder can easily be found using the method discussed in the previous section. To produce this mating pressure, the male member must have an outer radius greater than the inner radius of the female member. The difference in these two radii is called the interference δ, and is the radial deformation experienced by both cylinders at the interface. If a unit pressure is applied to the outer diameter of the male or inner cylinder, a decrease in the outer radius of δ_i results. Likewise, a unit

pressure applied to the inside of the female or outer member produces an increase in its inner radius of δ_o. Therefore, the reduction in interference per unit of interface pressure is given by

$$\delta_u = \delta_i + \delta_o \tag{28}$$

If the interference is at the i, i+1 layer interface,

$$\delta_u = -b(i)\cdot\epsilon_{\theta,b}(i) + a(i+1)\cdot\epsilon_{\theta,a}(i+1) \tag{29}$$

In general, however, the interference is small compared to b(i) and a(i+1), therefore

$$b(i) \doteq a(i+1) \tag{30}$$

and

$$\delta_u = b(i)\cdot[\epsilon_{\theta,a}(i+1) - \epsilon_{\theta,b}(i)] \tag{31}$$

The strains $\epsilon_{\theta,b}(i)$ and $\epsilon_{\theta,a}(i+1)$ are easily found from the procedure discussed in the previous section. Once this is done, the interference per unit of internal pressure must be scaled by pressure P_I to equal the total interference

$$\delta = P_I\cdot\delta_u \tag{32}$$

Thus, P_I is given by

$$P_I = \frac{\delta}{\delta_u} \tag{33}$$

P_I is the interface pressure that must exist to produce a radial deformation at the interface in both cylinders equal to the interference δ.

RESULTS

The multilayered solution was used to investigate the stress and strain distribution within a ten-layered cylinder (N=10). The cylinder had an inside radius a(1) = 1 inch and an outside radius b(10) = 2 inches, and each of the ten

layers was 0.1 inch thick. The material used was an IM6/epoxy with a 55 percent fiber-volume ratio. The layup considered consisted of five hoop-axial pairs starting at the inside radius of the cylinder. The material properties for the hoop and axial fiber orientations are given in Table I. The results generated consist of three sets of plots (Figures 3, 4, and 5). Each set of plots corresponds to one of three loading conditions. For each of these loading conditions, four graphs were generated displaying the stress and strain distribution within the cylinder as a function of radial position. These graphs include stresses in the r,θ,z directions and strains in the r,θ directions. The three loading conditions were unit internal pressure (p(1) = 1.0), unit external pressure (q(10) = 1.0), and a 1-microinch interference at the 5 to 6 layer interface.

TABLE I. MATERIAL PROPERTIES FOR IM6/EPOXY 55% FIBER-VOLUME RATIO

Fiber Direction	E_r (Mpsi)	E_θ (Mpsi)	E_z (Mpsi)	$\nu_{r\theta}$	$\nu_{\theta z}$	ν_{zr}
Hoop	1.126	23.31	1.126	0.0152	0.3147	0.3991
Axial	1.126	1.126	23.31	0.3991	0.0152	0.3147

The multilayered solution was also compared to a finite element solution for the cylinder with the first two loading conditions mentioned above. The ABAQUS finite element code was used to produce stress results used in the comparison. The finite element model contained 20 eight-node quadratic axisymmetric elements with two equal-sized elements used to model each of the ten orthotropic layers. The comparison was limited to the radial, hoop, and axial stress values evaluated at the inner and outer radii of each orthotropic layer. Tables II and III contain the results of this comparison.

TABLE II. COMPARISON BETWEEN MULTILAYERED SOLUTION AND ABAQUS FINITE ELEMENT SOLUTION USING 20 CAX8 ELEMENTS

Number of Layers N = 10, 5*(1-hoop, 1-axial), (see Table I)
a(1) = 1.0 in., b(10) = 2.0 in., p(1) = 1.0 psi, q(10) = 0.0 psi

Layer	Fiber Orient	Radius (in.)	Radial Stress (psi)		Hoop Stress (psi)		Axial Stress (psi)	
			Theory	ABAQUS	Theory	ABAQUS	Theory	ABAQUS
1	Hoop	1.0	-1.000	-0.993	5.477	5.481	-0.316	-0.313
		1.1	-0.495	-0.490	3.824	3.827	-0.139	-0.138
2	Axial	1.1	-0.495	-0.495	-0.006	-0.005	-0.158	-0.157
		1.2	-0.456	-0.456	-0.045	-0.045	-0.158	-0.157
3	Hoop	1.2	-0.456	-0.453	2.704	2.705	-0.141	-0.140
		1.3	-0.241	-0.239	2.037	2.038	-0.065	-0.065
4	Axial	1.3	-0.241	-0.241	0.006	0.006	-0.074	-0.074
		1.4	-0.224	-0.224	-0.011	-0.011	-0.074	-0.074
5	Hoop	1.4	-0.224	-0.223	1.550	1.550	-0.066	-0.066
		1.5	-0.117	-0.116	1.251	1.252	-0.028	-0.027
6	Axial	1.5	-0.117	-0.117	0.016	0.016	-0.032	-0.032
		1.6	-0.109	-0.109	0.008	0.007	-0.032	-0.032
7	Hoop	1.6	-0.109	-0.108	1.022	1.022	-0.028	-0.028
		1.7	-0.047	-0.046	0.883	0.883	-0.005	-0.005
8	Axial	1.7	-0.047	-0.047	0.025	0.025	-0.007	-0.007
		1.8	-0.043	-0.043	0.021	0.021	-0.007	-0.007
9	Hoop	1.8	-0.043	-0.043	0.773	0.772	-0.005	-0.005
		1.9	-0.002	-0.002	0.712	0.712	0.010	0.010
10	Axial	1.9	-0.002	-0.002	0.034	0.034	0.010	0.010
		2.0	0.000	0.000	0.032	0.032	0.010	0.010

TABLE III. COMPARISON BETWEEN MULTILAYERED SOLUTION AND ABAQUS FINITE ELEMENT SOLUTION USING 20 CAX8 ELEMENTS

Number of Layers N = 10, 5*(1-hoop, 1-axial), (see Table I)
a(1) = 1.0 in., b(10) = 2.0 in., p(1) = 0.0 psi, q(10) = 1.0 psi

Layer	Fiber Orient	Radius (in.)	Radial Stress (psi)		Hoop Stress (psi)		Axial Stress (psi)	
			Theory	ABAQUS	Theory	ABAQUS	Theory	ABAQUS
1	Hoop	1.0	0.000	-0.002	-2.650	-2.650	-0.040	-0.041
		1.1	-0.236	-0.237	-2.603	-2.603	-0.134	-0.134
2	Axial	1.1	-0.236	-0.236	-0.216	-0.216	-0.142	-0.142
		1.2	-0.234	-0.234	-0.218	-0.218	-0.142	-0.142
3	Hoop	1.2	-0.234	-0.235	-2.647	-2.647	-0.134	-0.134
		1.3	-0.428	-0.428	-2.890	-2.890	-0.215	-0.215
4	Axial	1.3	-0.428	-0.428	-0.304	-0.304	-0.230	-0.230
		1.4	-0.419	-0.419	-0.313	-0.312	-0.230	-0.230
5	Hoop	1.4	-0.419	-0.419	-3.134	-3.134	-0.215	-0.215
		1.5	-0.612	-0.612	-3.526	-3.526	-0.298	-0.298
6	Axial	1.5	-0.612	-0.612	-0.406	-0.406	-0.320	-0.320
		1.6	-0.600	-0.600	-0.418	-0.418	-0.320	-0.320
7	Hoop	1.6	-0.600	-0.600	-3.884	-3.885	-0.298	-0.298
		1.7	-0.807	-0.807	-4.379	-4.379	-0.388	-0.389
8	Axial	1.7	-0.807	-0.807	-0.522	-0.522	-0.418	-0.418
		1.8	-0.791	-0.791	-0.537	-0.537	-0.418	-0.418
9	Hoop	1.8	-0.791	-0.791	-4.820	-4.821	-0.389	-0.389
		1.9	-1.018	-1.018	-5.398	-5.399	-0.488	-0.488
10	Axial	1.9	-1.018	-1.018	-0.652	-0.652	-0.525	-0.526
		2.0	-1.000	-1.000	-0.670	-0.670	-0.525	-0.526

DISCUSSION

The stress and strain distributions for the three loading conditions are displayed in Figures 3, 4, and 5. In each case, the radial stress must be equal to the negative of the applied pressure at the loading surface. Therefore, for case 1 involving internal pressure, the radial stress was equal to -1.0 psi at the inside radius and zero at the outside radius. For case 2 involving external pressure, the radial stress was equal to -1.0 psi at the outside radius and zero at the inside radius. And for case 3, the radial stress was equal to zero at the inner and outer surfaces and equal to about -0.98 psi at the 5 to 6 layer interface, -0.98 was the interference pressure associated with the 1-microinch interference. In the three graphs showing the hoop stress distribution for the three loading conditions, it is clearly seen that the hoop layers took up most of the load. This is primarily due to the low radial stiffness of both the hoop and axial layers (ref 2). It is also observed that the axial stress for the three loading conditions was relatively small when compared to the hoop stress. This was expected because the axial stress was a second order effect related to the Poisson's contraction and axial stiffness of each layer. As a result of the combination of the low axial and radial stiffness of the hoop layer and the low radial stiffness of the axial layer, a very small axial load was needed to enforce the plane-strain boundary condition.

The graphs of the hoop strains for the three loading conditions show some interesting results. The hoop strain for the internal pressure loading was smooth and monotonically decreasing, while the hoop strain for the external pressure loading was smooth, but somewhat larger in magnitude a small distance away from the inner surface than at the inner surface. The hoop strain for the interference loading case shows a discontinuity at the interface of loading.

This was expected because the interference pressure causes a shrinking of the outer diameter of the inner cylinder and an expansion of the inner diameter of the outer cylinder. Finally, the radial strains for the three loading cases were not, in general, continuous. The radial strain for the interference loading shows this most clearly at a radial position of 1.6 inches. This is because the radial strain depended on both the material properties and stresses of each layer at the interface of each layer.

The theoretical and finite element comparisons of the radial, hoop, and axial stresses at the inner and outer surfaces of each orthotropic layer are shown in Tables II and III. Table II shows the comparison for the unit internal pressure loading case, and Table III shows the comparison for the unit external pressure loading case. For both loading cases, the comparison shows excellent agreement between the theory and the finite element results. For the finite element cases, the stresses were obtained at the nodes and are somewhat less accurate than stresses obtained at the integration points of the element.

CONCLUSION

A plane-strain elastic stress solution for a multiorthotropic-layered cylinder has been developed. The solution has been shown to be in excellent agreement with finite element results. The solution has also been implemented in a FORTRAN program to be used as a tool for the designer.

REFERENCES

1. S. G. Lekhnitskii, Theory of Elasticity of an Anisotropic Elastic Body, Holden-Day Inc., San Francisco, 1963.

2. G. P. O'Hara, "Some Results on Orthotropic Cylinders," ARDEC Technical Report, ARCCB-TR-87015, Benet Laboratories, Watervliet, NY, June 1987.

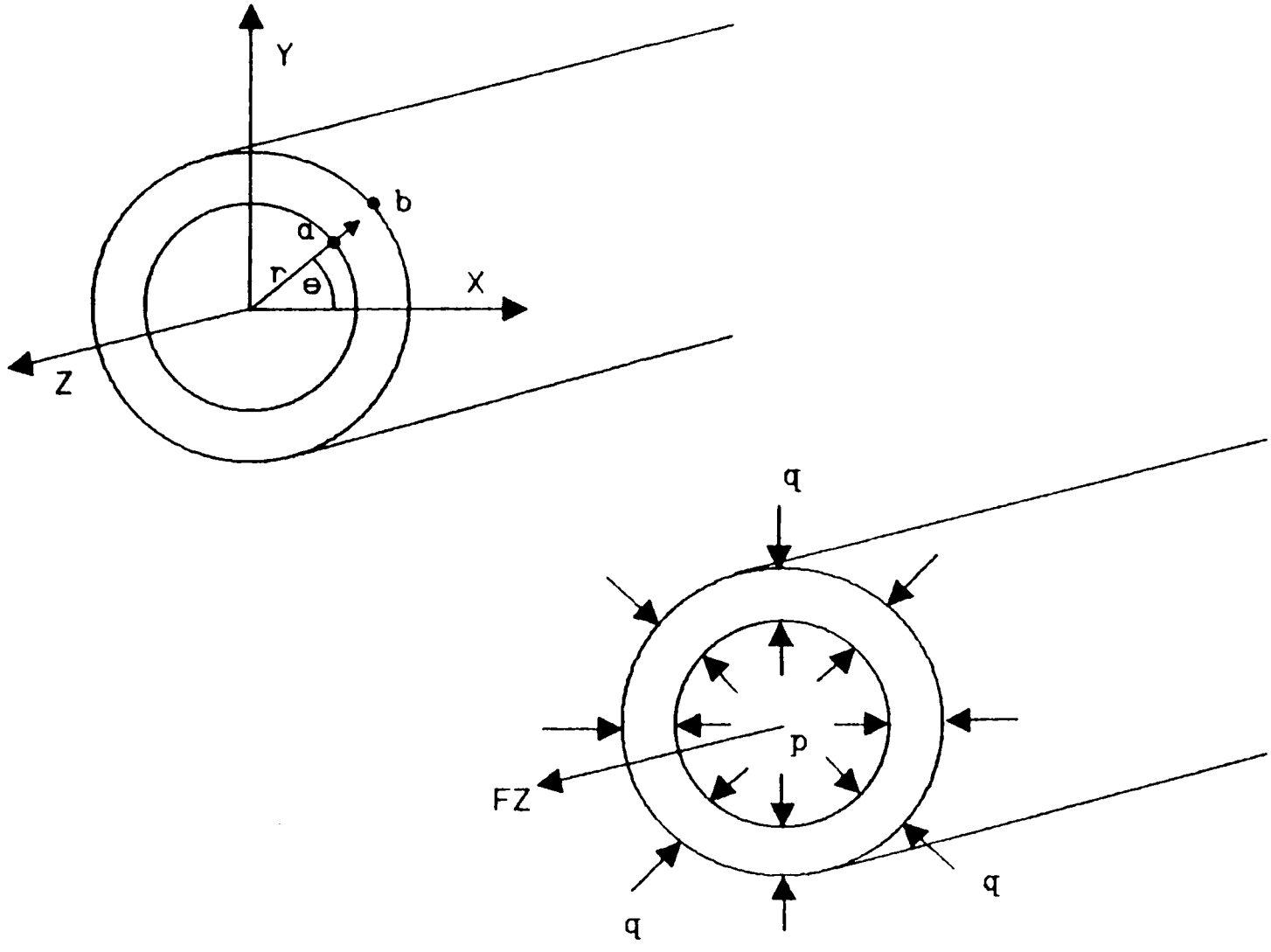

Figure 1 - Mono-layered Cylinder Geometry

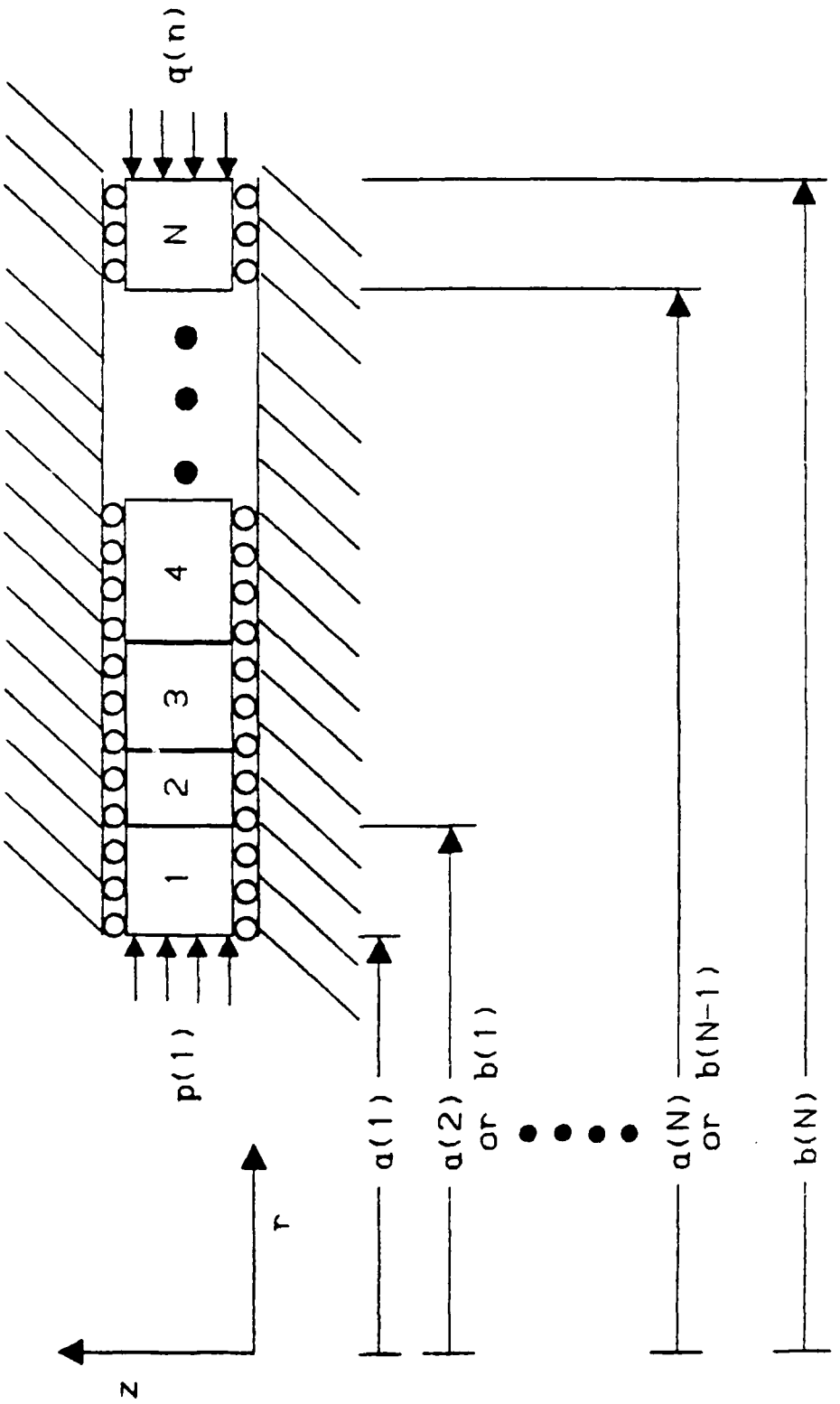

Figure 2 - Multi-layered Cylinder Geometry

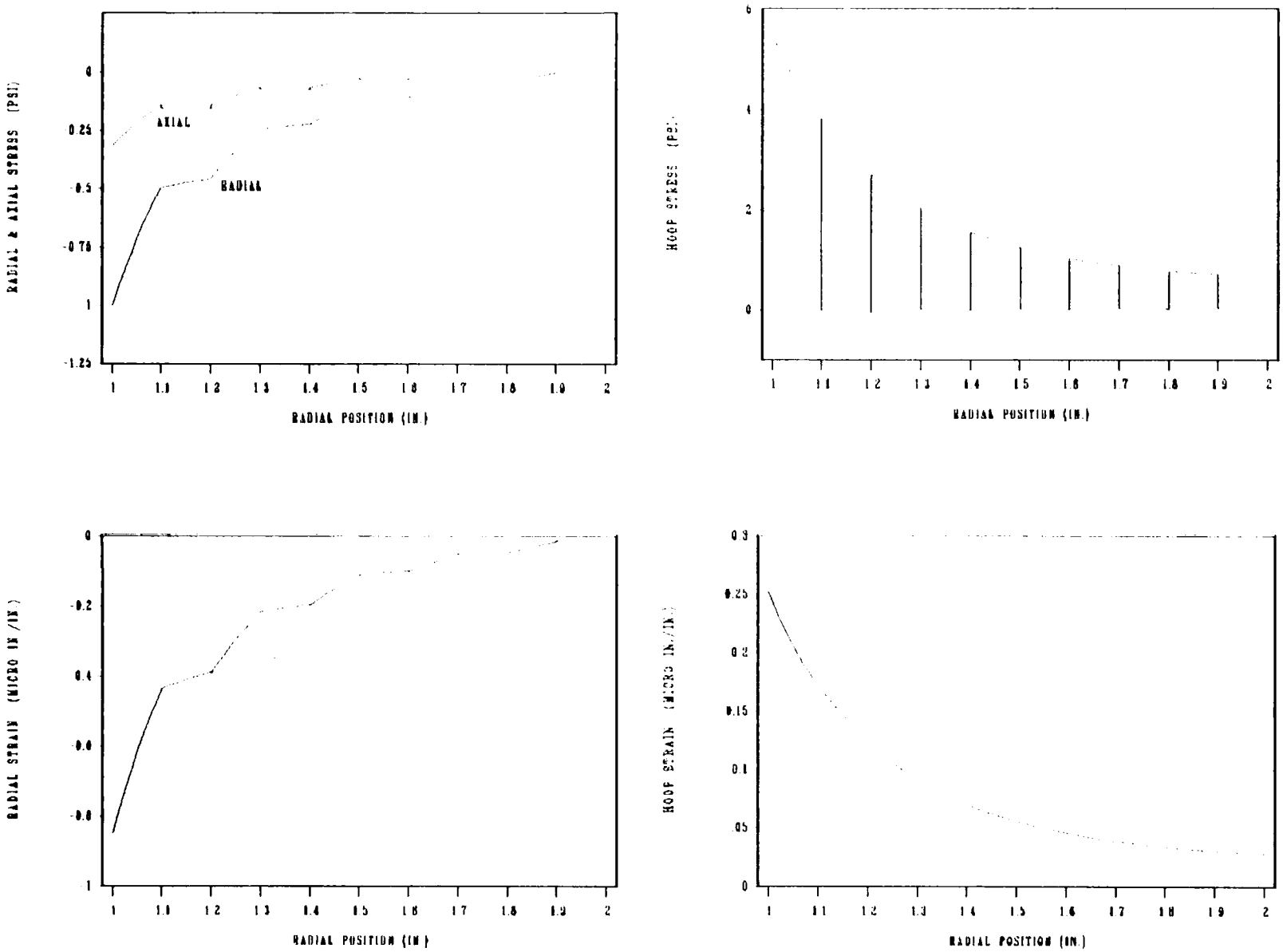

Figure 3. Theoretical stress and strain plots for N = 10, 5*(1-hoop, 1-axial), (see Table I), a(1) = 1.0 in., b(10) = 2.0 in., p(1) = 1.0 psi, q(10) = 0.0 psi.

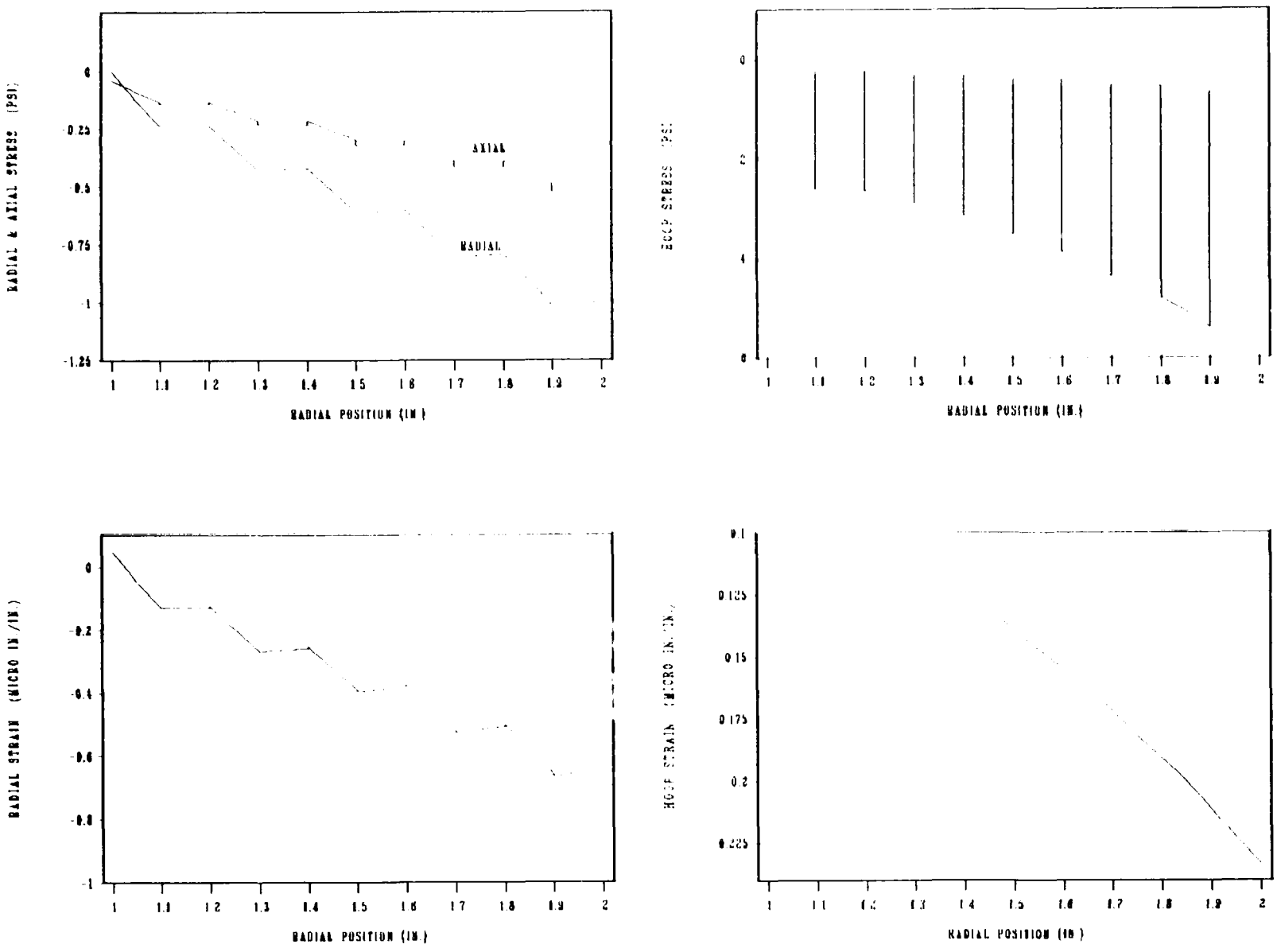

Figure 4. Theoretical stress and strain plots for N = 10, 5*(1-hoop, 1-axial), (see Table I), a(1) = 1.0 in., b(10) = 2.0 in., p(1) = 0.0 psi, q(10) = 1.0 psi.

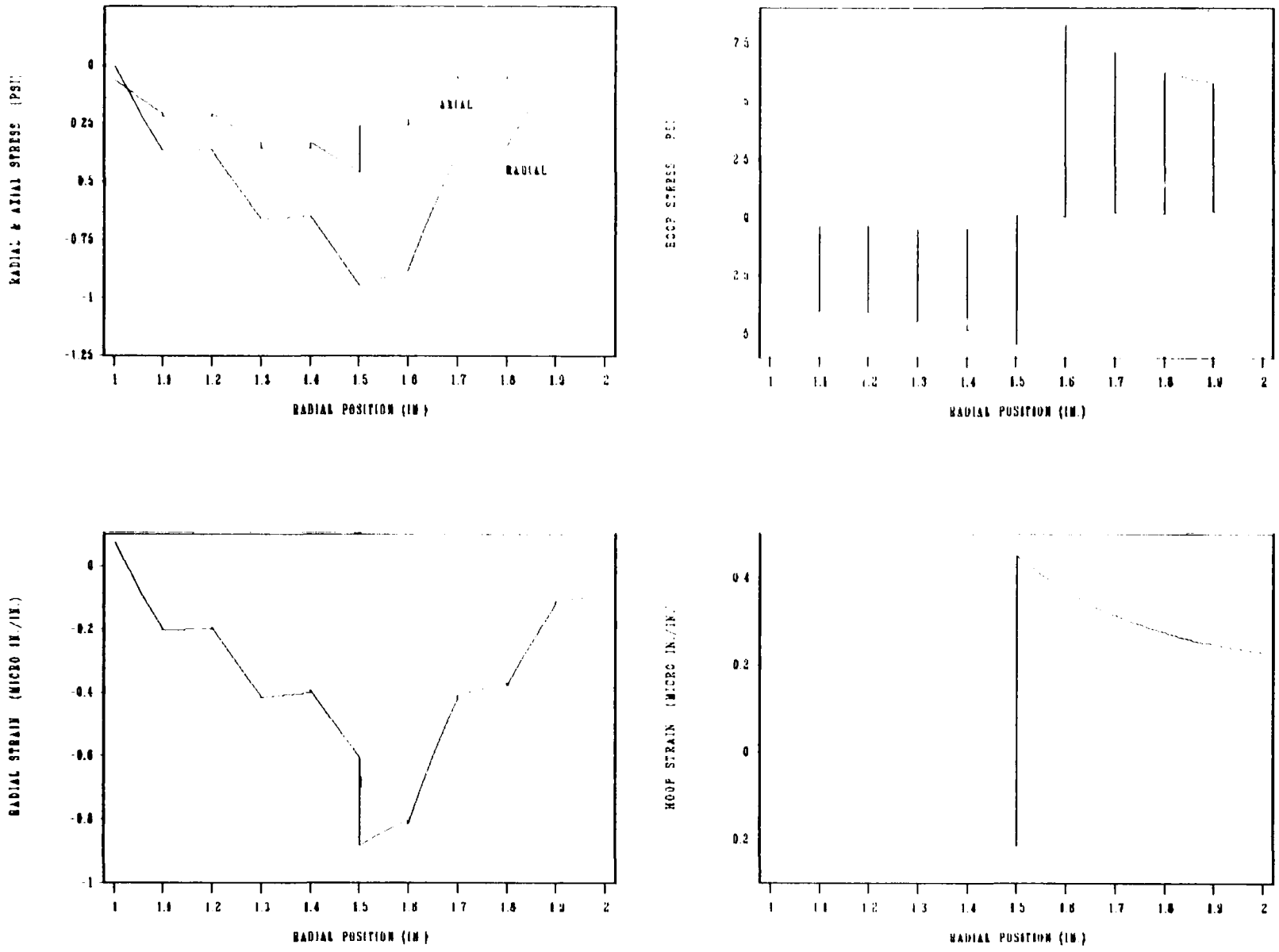

Figure 5. Theoretical stress and strain plots for N = 10, 5*(1-hoop, 1-axial) (see Table I), a(1) = 1.0 in., = 2.0 in., 1.0 μin. interference at the 5 to 6 layer interface.

TECHNICAL REPORT INTERNAL DISTRIBUTION LIST

	NO. OF COPIES
CHIEF, DEVELOPMENT ENGINEERING DIVISION	
ATTN: SMCAR-CCB-D	1
-DA	1
-DC	1
-DI	1
-DP	1
-DR	1
-DS (SYSTEMS)	1
CHIEF, ENGINEERING SUPPORT DIVISION	
ATTN: SMCAR-CCB-S	1
-SE	1
CHIEF, RESEARCH DIVISION	
ATTN: SMCAR-CCB-R	2
-RA	1
-RE	1
-RM	1
-RP	1
-RT	1
TECHNICAL LIBRARY ATTN: SMCAR-CCB-TL	5
TECHNICAL PUBLICATIONS & EDITING SECTION ATTN: SMCAR-CCB-TL	3
DIRECTOR, OPERATIONS DIRECTORATE ATTN: SMCWV-OD	1
DIRECTOR, PROCUREMENT DIRECTORATE ATTN: SMCWV-PP	1
DIRECTOR, PRODUCT ASSURANCE DIRECTORATE ATTN: SMCWV-QA	1

NOTE: PLEASE NOTIFY DIRECTOR, BENET LABORATORIES, ATTN: SMCAR-CCB-TL, OF ANY ADDRESS CHANGES.

TECHNICAL REPORT EXTERNAL DISTRIBUTION LIST

	NO. OF COPIES
ASST SEC OF THE ARMY RESEARCH AND DEVELOPMENT ATTN: DEPT FOR SCI AND TECH THE PENTAGON WASHINGTON, D.C. 20310-0103	1
ADMINISTRATOR DEFENSE TECHNICAL INFO CENTER ATTN: DTIC-FDAC CAMERON STATION ALEXANDRIA, VA 22304-6145	12
COMMANDER US ARMY ARDEC ATTN: SMCAR-AEE	1
SMCAR-AES, BLDG. 321	1
SMCAR-AET-O, BLDG. 351N	1
SMCAR-CC	1
SMCAR-CCP-A	1
SMCAR-FSA	1
SMCAR-FSM-E	1
SMCAR-FSS-D, BLDG. 94	1
SMCAR-IMI-I (STINFO) BLDG. 59 PICATINNY ARSENAL, NJ 07806-5000	2
DIRECTOR US ARMY BALLISTIC RESEARCH LABORATORY ATTN: SLCBR-DD-T, BLDG. 305 ABERDEEN PROVING GROUND, MD 21005-5066	1
DIRECTOR US ARMY MATERIEL SYSTEMS ANALYSIS ACTV ATTN: AMXSY-MP ABERDEEN PROVING GROUND, MD 21005-5071	1
COMMANDER HQ, AMCCOM ATTN: AMSMC-IMP-L ROCK ISLAND, IL 61299-6000	1
COMMANDER ROCK ISLAND ARSENAL ATTN: SMCRI-ENM ROCK ISLAND, IL 61299-5000	1
DIRECTOR US ARMY INDUSTRIAL BASE ENGR ACTV ATTN: AMXIB-P ROCK ISLAND, IL 61299-7260	1
COMMANDER US ARMY TANK-AUTMV R&D COMMAND ATTN: AMSTA-DDL (TECH LIB) WARREN, MI 48397-5000	1
COMMANDER US MILITARY ACADEMY ATTN: DEPARTMENT OF MECHANICS WEST POINT, NY 10996-1792	1
US ARMY MISSILE COMMAND REDSTONE SCIENTIFIC INFO CTR ATTN: DOCUMENTS SECT, BLDG. 4484 REDSTONE ARSENAL, AL 35898-5241	2
COMMANDER US ARMY FGN SCIENCE AND TECH CTR ATTN: DRXST-SD 220 7TH STREET, N.E. CHARLOTTESVILLE, VA 22901	1
COMMANDER US ARMY LABCOM MATERIALS TECHNOLOGY LAB ATTN: SLCMT-IML (TECH LIB) WATERTOWN, MA 02172-0001	2

NOTE: PLEASE NOTIFY COMMANDER, ARMAMENT RESEARCH, DEVELOPMENT, AND ENGINEERING CENTER, US ARMY AMCCOM, ATTN: BENET LABORATORIES, SMCAR-CCB-TL, WATERVLIET, NY 12189-4050, OF ANY ADDRESS CHANGES.

TECHNICAL REPORT EXTERNAL DISTRIBUTION LIST (CONT'D)

	NO. OF COPIES
COMMANDER US ARMY LABCOM, ISA ATTN: SLCIS-IM-TL 2800 POWDER MILL ROAD ADELPHI, MD 20783-1145	1
COMMANDER US ARMY RESEARCH OFFICE ATTN: CHIEF, IPO P.O. BOX 12211 RESEARCH TRIANGLE PARK, NC 27709-2211	1
DIRECTOR US NAVAL RESEARCH LAB ATTN: MATERIALS SCI & TECH DIVISION	1
CODE 26-27 (DOC LIB) WASHINGTON, D.C. 20375	1

	NO. OF COPIES
COMMANDER AIR FORCE ARMAMENT LABORATORY ATTN: AFATL/MN EGLIN AFB, FL 32542-5434	1
COMMANDER AIR FORCE ARMAMENT LABORATORY ATTN: AFATL/MNF EGLIN AFB, FL 32542-5434	1
METALS AND CERAMICS INFO CTR BATTELLE COLUMBUS DIVISION 505 KING AVENUE COLUMBUS, OH 43201-2693	1

NOTE: PLEASE NOTIFY COMMANDER, ARMAMENT RESEARCH, DEVELOPMENT, AND ENGINEERING CENTER, US ARMY AMCCOM, ATTN: BENET LABORATORIES, SMCAR-CCB-TL, WATERVLIET, NY 12189-4050, OF ANY ADDRESS CHANGES.